COBEM 2023 27TH INTERNATIONAL CONGRESS OF MECHANICAL ENGENEERING

ABCM Brazilian Society of Mechanical Sciences and Engineering
27th ABCM International Congress of Mechanical Engineering
December 04-08, 2023, Florianópolis-SC, Brazil

COB-2023-0110
EFFECTIVE FOURTH-ORDER ELASTICITY TENSOR OF PERIODIC POROUS MATERIALS BY A 3D COMPUTATIONAL HOMOGENIZATION PROCEDURE

Wanderson Ferreira dos Santos
Sergio Persival Baroncini Proença
Department of Structural Engineering, Sao Carlos School of Engineering, University of Sao Paulo. Address: Av. Trab. Sao Carlense, 400, Zip-Code: 13566-590,Sao Carlos, Sao Paulo, Brazil
e-mails: wanderson_santos@usp.br, persival@sc.usp.br

Abstract. *The evaluation of effective macroscopic constitutive behavior can be of particular interest in applications for non-homogeneous materials. In this context, this work addresses a framework based on the computational homogenization procedure implemented in ANSYS® Mechanical, Release 18.0 to predict the fourth-order elasticity tensor of periodic porous media. The process to impose the periodic boundary condition considering three-dimensional (3D) analysis is detailed. Periodic materials with unidirectional voids of circular cross-section are modeled with the concept of Representative Volume Element (RVE). Numerical simulations based on the Finite Element Method (FEM) are used to solve the Boundary Value Problem (BVP) for the RVE. An extrapolation strategy is explored to obtain the final results of the effective elastic constitutive tensor from the numerical results of the computational homogenization procedure. The results of this study are compared to analytical and numerical works reported in the literature. In summary, the computational approach provides responses in close agreement with the compared works.*

Keywords: *periodic porous materials, effective fourth-order elasticity tensor, computational homogenization, finite elements, extrapolation strategy.*

1. INTRODUCTION

Several materials found in engineering applications are non-homogeneous when viewed at lower scales, including composites and porous media. Therefore, the prediction of effective elastic constitutive properties can be important for material design in order to obtain the desired macroscopic properties. Some precursor works about effective elastic properties were Voigt (1889) (or upper bound) and Reuss (1929) (or lower bound). It is also worth mentioning the limits proposed by Hashin and Shtrikman (1963) with a formulation derived from variational principles. However, these analytical models rely on simplified assumptions and are applicable only to specific mixtures. Consequently, other works were developed over time to improve the prediction of the effective properties for non-homogeneous materials.

Numerous numerical strategies have been proposed to estimate the effective properties of periodic non-homogeneous materials. In particular, computational homogenization approaches using finite elements have been extensively explored in the literature. For example, Xia et al. (2003) showed an explicit unified form of boundary conditions for a periodic Representative Volume Element (RVE). Kari et al. (2007) performed a computational evaluation of the effective material properties for composites reinforced by randomly distributed spherical particles. Medeiros et al. (2012) proposed a method based on the development of numerical models of unit cells to predict the homogenized properties of intelligent composite materials with piezoelectric fibers. In a more recent context, Tian et al. (2019) provided a detailed numerical implementation algorithm for incorporating periodic boundary conditions to evaluate the effective mechanical properties of composites with intricate microstructures. Omairey et al. (2019) developed an ABAQUS® plug-in tool to estimate the homogenized effective elastic properties for user-created periodic RVEs. Zhu et al. (2020) conducted a comparative study on three techniques for computing macroscopic tangent moduli using a periodic homogenization scheme. Christoff et al. (2020) presented an ABAQUS® plug-in for estimation of the effective properties of cellular and composite materials with periodic structure using the Asymptotic Homogenization Method (AHM). Furthermore, Campillo et al. (2021) explored the Discrete Element Method (DEM) and the Finite Elements Method (FEM) combined with approximate periodic boundary conditions to estimate the elastic mechanical properties of open foams.

In this context, this paper evaluates the effective fourth-order elasticity tensor of a periodic porous materials by an approach based on computational homogenization. Some possible applications are in cellular materials and porous metals, for example. The computational homogenization procedure is implemented in ANSYS® Mechanical, Release 18.0, in which the process to impose the periodic boundary condition is described in detail. More specifically, a periodic porous material formed by unidirectional voids of circular cross-section is simulated with the concept of RVE (or unit cell). The final results of the effective elastic constitutive tensor are obtained with an extrapolation strategy based on a posteriori

estimation of error proposed by Szabó and Babuška (1991). In summary, the numerical results of the homogenization procedure for three different meshes are used to better estimate the final results of the effective elastic constitutive tensor. The results of this work are compared with the analytical solution proposed by Rodríguez-Ramos et al. (2013) and the numerical results in ABAQUS® obtained by Christoff et al. (2020). It is worth noting that this framework is an interesting tool for the design of non-homogeneous periodic materials.

2. COMPUTATIONAL HOMOGENIZATION PROCEDURE IN ANSYS® SOFTWARE

In this section, the methodology for obtaining the effective elastic constitutive tensor is shown in detail. Initially, some concepts about average-based homogenization theory are presented. Next, the computational homogenization procedure is described. The computational procedure consists of the following main steps: (i) defining the RVE morphology and the elastic properties of the matrix; (ii) creating the structured finite element mesh; (iii) imposing periodic boundary condition; (iv) solving the BVP for RVE with numerical simulations in finite elements; and (iv) post-processing the numerical results. Finally, the extrapolation strategy for estimating the components of the effective elastic constitutive tensor from the numerical results is indicated.

2.1 Average-based homogenization theory

The determination of the homogenized constitutive behavior can be necessary in the case of non-homogeneous materials. In this context, average-based homogenization theories are an interesting alternative for predicting effective (or homogenized) constitutive behavior. The macroscopic stress and strain fields ($\boldsymbol{\Sigma}$ and $\boldsymbol{E}$) are obtained based on the volume averaging of the microscopic strain and stress fields ($\boldsymbol{\sigma}$ and $\boldsymbol{\varepsilon}$) over a local RVE (Bishop and Hill, 1951):

$$\boldsymbol{\Sigma} = \frac{1}{V}\int_V \boldsymbol{\sigma} dV = \langle \boldsymbol{\sigma} \rangle , \tag{1}$$

$$\boldsymbol{E} = \frac{1}{V}\int_V \boldsymbol{\varepsilon} dV = \langle \boldsymbol{\varepsilon} \rangle , \tag{2}$$

respectively.

The Hill-Mandel Principle of Macro-Homogeneity establishes the association between the macroscale and microscale (Bishop and Hill, 1951; Mandel, 1971). This principle assumes that the macroscopic stress power must equal the volume average of the microscopic stress power over the RVE:

$$\boldsymbol{\Sigma} : \boldsymbol{E} = \frac{1}{V}\int_V \boldsymbol{\sigma} : \boldsymbol{\varepsilon}\, dV = \langle \boldsymbol{\sigma} : \boldsymbol{\varepsilon} \rangle . \tag{3}$$

Macroscopic strain and stress fields are associated by the constitutive law considering the fourth-order effective elastic tensor ($\underline{\mathbf{C}}$):

$$\boldsymbol{\Sigma} = \underline{\mathbf{C}} : \boldsymbol{E} , \tag{4}$$

or in index notation:

$$\Sigma_{ij} = C_{ijkl} E_{kl} . \tag{5}$$

The macroscopic constitutive law can be written in terms of the following expanded matrix notation form:

$$\begin{Bmatrix} \Sigma_{11} \\ \Sigma_{22} \\ \Sigma_{33} \\ \Sigma_{12} \\ \Sigma_{23} \\ \Sigma_{13} \end{Bmatrix} = \begin{bmatrix} C_{1111} & C_{1122} & C_{1133} & C_{1112} & C_{1123} & C_{1113} \\ C_{1122} & C_{2222} & C_{2233} & C_{2212} & C_{2223} & C_{2213} \\ C_{1133} & C_{2233} & C_{3333} & C_{3312} & C_{3323} & C_{1213} \\ C_{1112} & C_{2212} & C_{3312} & C_{1212} & C_{1223} & C_{1213} \\ C_{1123} & C_{2223} & C_{3323} & C_{1223} & C_{2323} & C_{2313} \\ C_{1113} & C_{2213} & C_{1213} & C_{1213} & C_{2313} & C_{1313} \end{bmatrix} \begin{Bmatrix} E_{11} \\ E_{22} \\ E_{33} \\ 2E_{12} \\ 2E_{23} \\ 2E_{13} \end{Bmatrix} . \tag{6}$$

2.2 Material properties

The material is a periodic porous media composed of unidirectional voids of circular cross-section (see Fig. 1). Due to the periodicity of the material, the analyses can be performed considering the concept of RVE (or unit cell). Three different porosity volume fractions (0.2, 0.35 and 0.55) are evaluated. The microscopic elastic properties of the matrix are adopted according to Rodríguez-Ramos et al. (2013): (i) $Y_m = 70GPa$ (elasticity modulus); (ii) $\nu = 0.3$ (Poisson's coefficient). All results are compared with the analytical solution proposed by Rodríguez-Ramos et al. (2013). In addition, the final results are also compared with the numerical results obtained in ABAQUS® by Christoff et al. (2020).

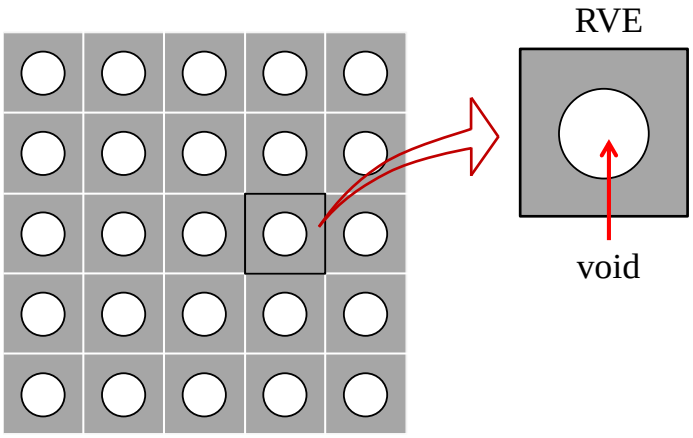

Figure 1. Periodic porous media with unidirectional voids of circular cross-section.

2.3 Periodic boundary conditions in 3D analysis using ANSYS® software

To understand the periodic condition, let us consider the two-dimensional representation of Fig. 2. Note that the contour is formed by positive and negative parts (Γ_i^+ and Γ_i^-) with respective unit normals (n^+ and n^-). In this context, each point of the positive part ($\boldsymbol{x}^+$) can be associated with the opposite point of the negative part ($\boldsymbol{x}^-$).

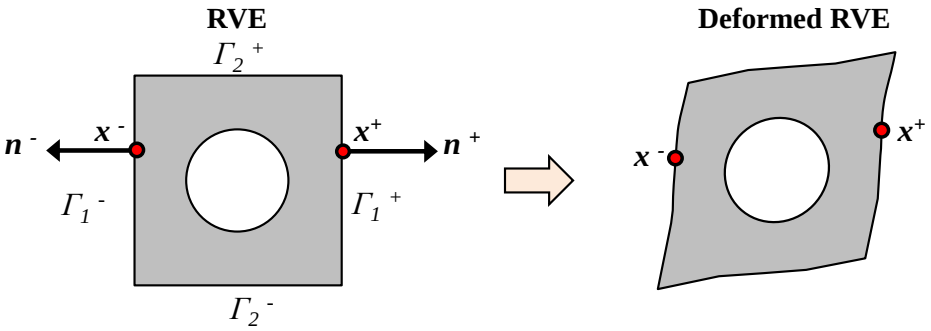

Figure 2. Periodic RVE.

The previous considerations are important to understand the periodic condition given in the general form by:

$$\boldsymbol{u} = \boldsymbol{E}^* \cdot \boldsymbol{x} + \tilde{\boldsymbol{u}} \quad \forall \quad \boldsymbol{x} \in \partial V \,, \tag{7}$$

where $\tilde{\boldsymbol{u}}$ is called periodic fluctuation and $\boldsymbol{E}^*$ is the macroscopic homogeneous strain tensor imposed on the outer contour of the RVE.

Fluctuations are periodic on the contour. Thus, the fluctuation of $\boldsymbol{x}^+$ is equal to the fluctuation of $\boldsymbol{x}^-$ on the contour:

$$\tilde{\boldsymbol{u}}(\boldsymbol{x}^+) = \tilde{\boldsymbol{u}}(\boldsymbol{x}^-) \,. \tag{8}$$

Furthermore, the following condition must be satisfied for the external surface traction:

$$\boldsymbol{\sigma}\cdot\boldsymbol{n}^{+} = \boldsymbol{\sigma}\cdot\boldsymbol{n}^{-} \quad \forall \quad \boldsymbol{x}\in\partial V\,, \tag{9}$$

where $\boldsymbol{n}^{-} = -\boldsymbol{n}^{+}$.

After some deductions, we can also conclude that:

$$\boldsymbol{E} = \langle\boldsymbol{\varepsilon}\rangle = \boldsymbol{E}^{*}\,. \tag{10}$$

The periodic fluctuation portion ($\tilde{\boldsymbol{u}}$) is not known initially in the problem. An alternative to impose the periodic condition is to associate the displacements of the corresponding opposite nodes. In this sense, the displacements of opposite nodes ($\boldsymbol{x}^{+}$ and $\boldsymbol{x}^{-}$) can be written as follows:

$$\boldsymbol{u}^{+} = \boldsymbol{E}^{*}\cdot\boldsymbol{x}^{+} + \tilde{\boldsymbol{u}}\left(\boldsymbol{x}^{+}\right), \tag{11a}$$

$$\boldsymbol{u}^{-} = \boldsymbol{E}^{*}\cdot\boldsymbol{x}^{-} + \tilde{\boldsymbol{u}}\left(\boldsymbol{x}^{-}\right). \tag{11b}$$

Therefore, Eqs. (11a) and (11b) can be used to create a constraint equation that must be added to the Boundary Value Problem (BVP):

$$\boldsymbol{u}^{+} - \boldsymbol{u}^{-} = \boldsymbol{E}^{*}\cdot\left(\boldsymbol{x}^{+} - \boldsymbol{x}^{-}\right). \tag{12}$$

The previously presented concept can be extended to impose the periodic boundary condition in 3D analyses. In this case, let us consider Fig. 3. Note that the RVE contour is formed by sets of corners (S_{corner}), edges (S_{edge}) and faces (S_{face}). Such sets can be conveniently correlated to create constraint equations in the Boundary Value Problem (BVP). The sets that must be correlated are indicated below:

$$S_{face} = \left\{(BCGF, ADHE);(ABCD, EFGH);(ABFE, DCGH)\right\}, \tag{13}$$

$$S_{edge} = \begin{Bmatrix}(BF,CG);(BF,AE);(AE,DH);(AB,CD);(AB,EF);(EF,GH);\\(BC,AD);(BC,FG);(FG,EH);(AD,EH);(CD,GH);(CG,DH)\end{Bmatrix}, \tag{14}$$

$$S_{corner} = \begin{Bmatrix}(B,C);(C,G);(G,F);(A,G);(D,H);(H,E);\\(E,F);(B,A);(A,E);(B,F);(C,D);(G,H)\end{Bmatrix}. \tag{15}$$

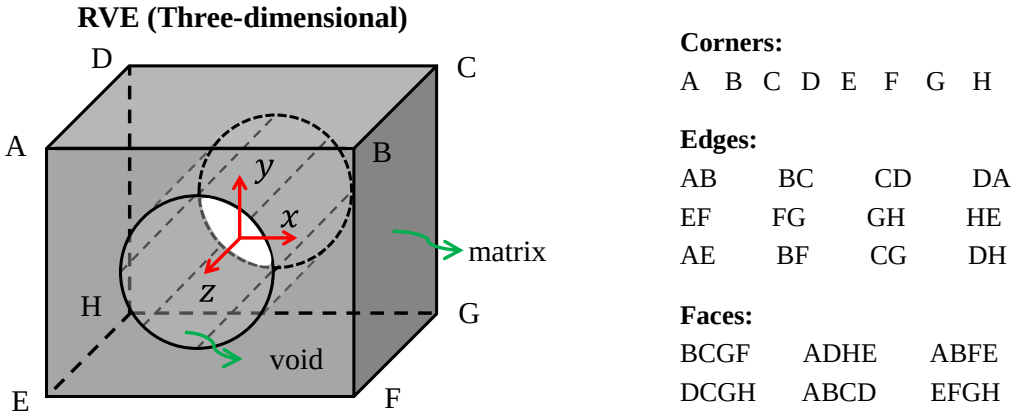

Figure 3. 3D RVE with indication of corners, edges and faces.

Furthermore, we explored the Ansys Parametric Design Language (APDL) to define the constraint equations in numerical simulations using Ansys® software.

2.4 Post-processing of results in ANSYS® software

The last step of the computational homogenization procedure is the post-processing. In this case, the stress average value (Σ) can be calculated by following expression:

$$\Sigma = \langle \boldsymbol{\sigma} \rangle = \frac{1}{V} \sum_{i=1}^{nel} \boldsymbol{\sigma}_i V_i \ , \tag{16}$$

where nel is the number of the finite elements; V_i is the volume of the i element; $\boldsymbol{\sigma}_i$ is the stress tensor evaluated for the i element; V is the unit cell volume.

Furthermore, the strain average value ($\boldsymbol{E}$) is given by:

$$\boldsymbol{E} = \boldsymbol{E}^* . \tag{17}$$

The macroscopic constitutive behavior is assumed to be linear elastic obeying an orthotropic law. In this case, the macroscopic constitutive law considering the stiffness tensor ($\underline{\boldsymbol{C}}$) can be represented in a simplified form as:

$$\begin{Bmatrix} \Sigma_{11} \\ \Sigma_{22} \\ \Sigma_{33} \\ \Sigma_{12} \\ \Sigma_{23} \\ \Sigma_{13} \end{Bmatrix} = \begin{bmatrix} C_{1111} & C_{1122} & C_{1133} & 0 & 0 & 0 \\ C_{1122} & C_{2222} & C_{2233} & 0 & 0 & 0 \\ C_{1133} & C_{2233} & C_{3333} & 0 & 0 & 0 \\ 0 & 0 & 0 & C_{1212} & 0 & 0 \\ 0 & 0 & 0 & 0 & C_{2323} & 0 \\ 0 & 0 & 0 & 0 & 0 & C_{1313} \end{bmatrix} \begin{Bmatrix} E_{11} \\ E_{22} \\ E_{33} \\ 2E_{12} \\ 2E_{23} \\ 2E_{13} \end{Bmatrix} . \tag{18}$$

The components of are obtained from the results of and using the Eq. (18). In this sense, six loading situations are necessary to define all components of the effective elastic constitutive tensor for the RVE:

$$E_{11} = 1.0, \qquad E_{22} = E_{33} = 2E_{12} = 2E_{13} = 2E_{23} = 0.0 \ , \tag{19a}$$

$$E_{22} = 1.0, \qquad E_{11} = E_{33} = 2E_{12} = 2E_{13} = 2E_{23} = 0.0 \ , \tag{19b}$$

$$E_{33} = 1.0, \qquad E_{11} = E_{22} = 2E_{12} = 2E_{13} = 2E_{23} = 0.0 \ , \tag{19c}$$

$$2E_{12} = 1.0, \qquad E_{11} = E_{22} = E_{33} = 2E_{13} = 2E_{23} = 0.0 \ , \tag{19d}$$

$$2E_{13} = 1.0, \qquad E_{11} = E_{22} = E_{33} = 2E_{12} = 2E_{23} = 0.0 \ , \tag{19e}$$

$$2E_{23} = 1.0, \qquad E_{11} = E_{22} = E_{33} = 2E_{12} = 2E_{13} = 0.0 \ . \tag{19f}$$

2.5 Strategy to estimate effective elastic constitutive tensor from numerical results

In order to obtain better precision in the final results, an extrapolation strategy is explored in this work based on the formulation proposed by Szabó and Babuška (1991). In summary, Szabó and Babuška (1991) presented an approach for posterior estimation of error in energy norm using the results of three distinct meshes (p, $p-1$ and $p-2$) in finite element simulations. The initial approach is extended in this work to study the components of the effective elastic constitutive tensor. More specifically, the final result of the component (C_{ijkl}) is obtained by the following expression:

$$\frac{C_{ijkl} - C_{ijkl}^{(p)}}{C_{ijkl} - C_{ijkl}^{(p-1)}} \approx \left(\frac{C_{ijkl} - C_{ijkl}^{(p-1)}}{C_{ijkl} - C_{ijkl}^{(p-2)}} \right)^{Q} , \tag{20}$$

with

$$Q = \frac{\log\left(\frac{N^{(p-1)}}{N^{(p)}}\right)}{\log\left(\frac{N^{(p-2)}}{N^{(p-1)}}\right)}, \tag{21}$$

where N is the number of degrees of freedom of the mesh (D.F).

In this work, numerical results were obtained for four different meshes to compare the numerical results. The 20-node hexahedral finite element was used in numerical simulations. The meshes are shown in Figs. 4, 5 and 6. More data on the meshes are presented in Tab. 1. According to Tab. 1, Mesh 1 is the least refined and Mesh 2 is the most refined. It is worth noting that the numerical results of three different meshes are necessary to predict the final result of C_{ijkl}. In this context, the three most refined meshes (Meshes 2, 3 and 4) were used to extrapolate the numerical results. In addition, the meshes are structured, which avoids error propagation in preferred directions.

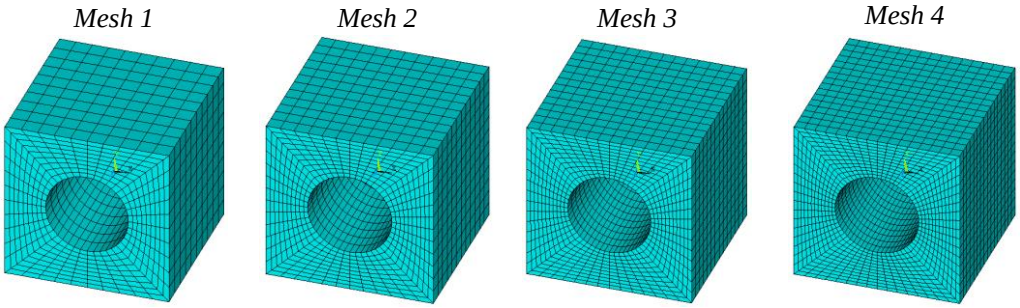

Figure 2. Meshes for $f = 0.20$.

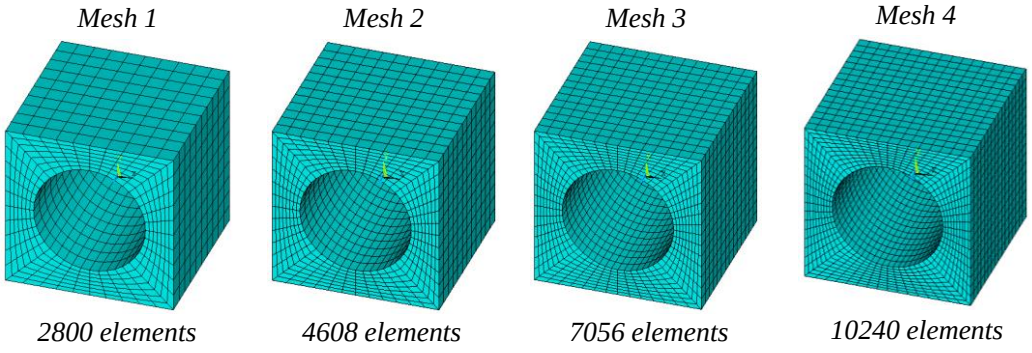

Figure 2. Meshes for $f = 0.35$.

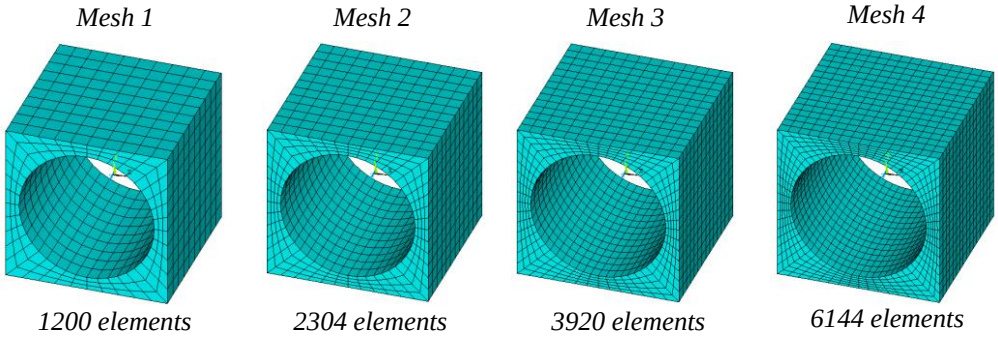

Figure 2. Meshes for $f = 0.55$.

Table 1. Mesh data used in numerical simulations in finite elements.

Porosity	Mesh 1			Mesh 2			Mesh 3			Mesh 4		
	Elem.	Nodes	D.F.	Elem.	Nodes	D.F.	Elem.	Nodes	D.F.	Elem.	Nodes	D.F.
$f = 0.20$	3600	16760	50280	5760	26304	78912	8624	38808	116424	12288	54656	163968
$f = 0.35$	2800	13320	39960	4608	21408	64224	7056	32200	96600	10240	46080	138240
$f = 0.55$	1200	6440	19320	2304	11616	34848	3920	18984	56952	6144	28928	86784

3. RESULTS AND DISCUSSION

This section comprises: (i) numerical results computed from the computational homogenization procedure (ii) final results obtained by the extrapolation strategy using the Eq. (20).

3.1 Numerical results of the computational homogenization procedure

The numerical results of the effective elastic constitutive tensor obtained by the computational homogenization procedure for $f = 0.20$, $f = 0.35$ and $f = 0.55$ are presented in Tabs. 2, 3 and 4, respectively. Mesh 1 is the least refined and Mesh 4 is the most refined. The comparison of the results for the different meshes is performed by the relative difference in modulus. In this context, the relative difference ($Diff$) from Mesh B to Mesh A is given by:

$$Diff = \left| \frac{C_{ijkl}^{(A)} - C_{ijkl}^{(B)}}{C_{ijkl}^{(A)}} \right| 100\% . \tag{22}$$

Table 2. Numerical results of the effective elastic constitutive tensor obtained by the computational homogenization procedure for $f = 0.20$.

Component	Mesh 1	Mesh 2	Mesh 3	Mesh 4	Relative differences in module		
	(1)	(2)	(3)	(4)	(2) to (1)	(3) to (2)	(4) to (3)
C_{1111} (GPa)	53.3760	53.3801	53.3826	53.3843	0.0076%	0.0048%	0.0032%
C_{3333} (GPa)	68.9172	68.9171	68.9169	68.9169	0.0003%	0.0002%	0.0001%
C_{1122} (GPa)	18.3843	18.3793	18.3761	18.3740	0.0275%	0.0171%	0.0114%
C_{1133} (GPa)	21.5281	21.5278	21.5276	21.5275	0.0014%	0.0008%	0.0005%
C_{1212} (GPa)	13.4466	13.4398	13.4355	13.4327	0.0506%	0.0314%	0.0210%
C_{1313} (GPa)	17.9457	17.9456	17.9455	17.9454	0.0007%	0.0004%	0.0003%

Table 3. Numerical results of the effective elastic constitutive tensor obtained by the computational homogenization procedure for $f = 0.35$.

Component	Mesh 1	Mesh 2	Mesh 3	Mesh 4	Relative differences in module		
	(1)	(2)	(3)	(4)	(2) to (1)	(3) to (2)	(4) to (3)
C_{1111} (GPa)	36.5315	36.5344	36.5362	36.5374	0.0079%	0.0050%	0.0033%
C_{3333} (GPa)	53.8456	53.8448	53.8443	53.8439	0.0016%	0.0009%	0.0006%
C_{1122} (GPa)	9.8092	9.8017	9.7971	9.7940	0.0766%	0.0469%	0.0309%
C_{1133} (GPa)	13.9022	13.9008	13.9000	13.8994	0.0099%	0.0060%	0.0039%
C_{1212} (GPa)	6.6491	6.6401	6.6345	6.6309	0.1355%	0.0831%	0.0547%
C_{1313} (GPa)	12.9197	12.9189	12.9185	12.9182	0.0062%	0.0037%	0.0024%

Table 4. Numerical results of the effective elastic constitutive tensor obtained by the computational homogenization procedure for $f = 0.55$.

Component	Mesh 1	Mesh 2	Mesh 3	Mesh 4	Relative differences in module		
	(1)	(2)	(3)	(4)	(2) to (1)	(3) to (2)	(4) to (3)
C_{1111} (GPa)	20.5207	20.5148	20.5112	20.5089	0.0287%	0.0173%	0.0113%
C_{3333} (GPa)	35.8105	35.8076	35.8059	35.8047	0.0082%	0.0048%	0.0031%
C_{1122} (GPa)	3.4118	3.4016	3.3956	3.3917	0.2986%	0.1769%	0.1135%
C_{1133} (GPa)	7.1797	7.1749	7.1720	7.1702	0.0672%	0.0400%	0.0258%
C_{1212} (GPa)	1.8360	1.8271	1.8221	1.8190	0.4830%	0.2748%	0.1724%
C_{1313} (GPa)	7.4728	7.4688	7.4664	7.4649	0.0534%	0.0315%	0.0203%

In general, the results are close when comparing the meshes. The biggest differences are observed for the C_{1212} component. It is also worth mentioning the differences in the case of the component. The increase in mesh refinement provides a reduction of the differences in results, indicating mesh convergence for the effective properties.

3.2 Final results after the extrapolation strategy

The final results of the effective elastic constitutive tensor after the extrapolation strategy for $f = 0.20$, $f = 0.35$ and $f = 0.55$ are shown in Tables 5, 6 and 7, respectively. The extrapolated results are compared with the analytical solution proposed by Rodríguez-Ramos et al. (2013) and the numerical results in ABAQUS® obtained by Christoff et al. (2020). The numerical results obtained with the most refined mesh (Mesh 4) are also presented for comparison with the final results of the extrapolation strategy. Note that relative differences in module are also shown.

Table 5. Final results of the effective elastic constitutive tensor obtained with the extrapolation strategy for $f = 0.20$.

	Rodríguez-Ramos et al. (2013)	Christoff et al. (2020)	Authors: Mesh 4	Authors: Extrapolation	Relative differences in module		
Component	(1)	(2)	(3)	(4)	(2) to (1)	(3) to (1)	(4) to (1)
C_{1111} (GPa)	53.3900	53.5194	53.3843	53.3905	0.2423%	0.0106%	0.0009%
C_{3333} (GPa)	68.9161	68.9768	68.9169	68.9167	0.0882%	0.0011%	0.0009%
C_{1122} (GPa)	18.3660	18.4004	18.3740	18.3673	0.1874%	0.0438%	0.0071%
C_{1133} (GPa)	21.5268	21.5759	21.5275	21.5274	0.2280%	0.0033%	0.0028%
C_{1212} (GPa)	13.4221	13.5327	13.4327	13.4241	0.8247%	0.0792%	0.0149%
C_{1313} (GPa)	17.9451	17.9761	17.9454	17.9446	0.1732%	0.0018%	0.0028%

Table 6. Final results of the effective elastic constitutive tensor obtained with the extrapolation strategy for $f = 0.35$.

	Rodríguez-Ramos et al. (2013)	Christoff et al. (2020)	Authors: Mesh 4	Authors: Extrapolation	Relative differences in module		
Component	(1)	(2)	(3)	(4)	(2) to (1)	(3) to (1)	(4) to (1)
C_{1111} (GPa)	36.5360	36.659	36.5374	36.5415	0.3361%	0.0038%	0.0151%
C_{3333} (GPa)	53.8371	53.912	53.8439	53.8395	0.1391%	0.0127%	0.0045%
C_{1122} (GPa)	9.7811	9.806	9.7940	9.7829	0.2511%	0.1323%	0.0186%
C_{1133} (GPa)	13.8951	13.939	13.8994	13.8956	0.3181%	0.0312%	0.0036%
C_{1212} (GPa)	6.6163	6.694	6.6309	6.6202	1.1760%	0.2207%	0.0592%
C_{1313} (GPa)	12.9153	12.951	12.9182	12.9163	0.2790%	0.0221%	0.0077%

Table 7. Final results of the effective elastic constitutive tensor obtained with the extrapolation strategy for $f = 0.55$.

	Rodríguez-Ramos et al. (2013)	Christoff et al. (2020)	Authors: Mesh 4	Authors: Extrapolation	Relative differences in module		
Component	**(1)**	**(2)**	**(3)**	**(4)**	**(2) to (1)**	**(3) to (1)**	**(4) to (1)**
C_{1111} (GPa)	20.4986	20.4986	20.5089	20.5015	0.2602%	0.0503%	0.0141%
C_{3333} (GPa)	35.7979	35.7979	35.8047	35.7986	0.1155%	0.0191%	0.0020%
C_{1122} (GPa)	3.3787	3.3787	3.3917	3.3783	0.2782%	0.3862%	0.0127%
C_{1133} (GPa)	7.1632	7.1632	7.1702	7.1650	0.2627%	0.0977%	0.0251%
C_{1212} (GPa)	1.8088	1.8088	1.8190	1.8101	1.0431%	0.5631%	0.0708%
C_{1313} (GPa)	7.4591	7.4591	7.4649	7.4605	0.2739%	0.0778%	0.0182%

The numerical results obtained with Mesh 4 are close to the literature references. In general, the extrapolation strategy provided a reduction of differences in comparison with the analytical approach proposed by Rodríguez-Ramos et al. (2013). More specifically, all differences are less than 0.1% after using the extrapolation strategy. It is worth mentioning that a positive aspect of approaches based on numerical simulations is the possibility of simulating RVEs with different morphologies, properties, and porosities in an analogous way. Therefore, the framework of this work can be interesting for estimating the effective elastic constitutive tensor of periodic porous solids.

4. CONCLUSIONS

This paper addressed the effective elastic tensor of periodic porous media by using a framework based on a computational homogenization procedure implemented in ANSYS® Mechanical, Release 18.0. In particular, periodic materials with unidirectional voids of circular cross-section were investigated. Numerical simulations with finite elements were computed to predict the numerical results of the effective elastic tensor. An extrapolation strategy was explored to provide more accurate results of the effective elastic tensor from numerical results.

The numerical results obtained from the computational homogenization procedure demonstrated a close agreement with the analytical and numerical results reported in the literature. It is worth mentioning that the computational framework coupled with the extrapolation strategy yielded effective properties that closely aligned with the analytical approach. Therefore, the extrapolation strategy provided an improvement in the accuracy of the numerical results.

Finally, the computational homogenization procedure implemented in ANSYS® software is an interesting tool for the design of periodic porous media. This approach offers the advantage of enabling convenient modifications to parameters such as RVE morphology, material properties, and porosity. Furthermore, this computational strategy can be easily extended to assess periodic composite materials.

5. ACKNOWLEDGEMENTS

The authors would like to gratefully acknowledge Coordination for the Improvement of Higher Education Personnel (CAPES-Brazil) for the financial support.

6. REFERENCES

ANSYS® Mechanical, Release 18.0, “https://www.ansys.com”.

Bishop, J.F.W. and Hill, R., 1951, “Prediction of composite properties from a representative volume element” Philosophical Magazine Series 5, Vol.42, pp. 414-427.

Campillo, M., Sedaghati, R., Drew, R. A.L., Alfonso, I. and Pérez, L., 2021, “Development of an RVE using a DEM–FEM scheme under modified approximate periodic boundary condition to estimate the elastic mechanical properties of open foams”, Engineering with Computers, Vol.38, pp. 1767-1785.

Christoff, B.G., Brito-Santana, H., Talreja, R. and Tita, V., 2020, “Development of an ABAQUS plug-in to evaluate the fourth-order elasticity tensor of a periodic material via homogenization by the asymptotic expansion method”, Finite Elements in Analysis and Design, Vol.181, pp. 1-13.

Kari, S., Berger, H., Rodriguez-Ramos, R. and Gabbert, U., 2007, “Computational evaluation of effective material properties of composites reinforced by randomly distributed spherical particles”, Composite Structures, Vol.77, pp. 223-231.

Mandel, J., 1971, “Plasticité classique et viscoplasticité”, Udine, Springer-Verlag.

Medeiros, R., Moreno, M.E., Marques, F.D. and Tita, V., 2012, “Effective properties evaluation for smart composite materials”, Journal of the Brazilian Society of Mechanical Sciences and Engineering, Vol.34, pp. 362-370.

Omairey, S.L., Dunning, P. D. and Sriramula, S., 2019, "Development of an ABAQUS plugin tool for periodic RVE homogenization", Engineering with Computers, Vol.35, pp. 567-577.

Rodríguez-Ramos, R., Medeiros, R., Guinovart-Díaz, R., Bravo-Castillero, J., Otero, J. A. and Tita, V., 2013, "Different approaches for calculating the effective elastic properties in composite materials under imperfect contact adherence", Composite Structures, Vol.99, pp. 264-275.

Szabó, B. and Babuška, I., 1991, "Finite element analysis", New York , Wiley-Interscience.

Tian, W., Qi, L., Chao, X., Liang, J. and Fu, M., 2019, "Periodic boundary condition and its numerical implementation algorithm for the evaluation of effective mechanical properties of the composites with complicated micro-structures", Composites Part B: Engineering, Vol.162, pp. 1-10.

Xia, Z., Zhang, Y. and Ellyin, F., 2003, "A unified periodical boundary conditions for representative volume elements of composites and applications", International Journal of Solids and Structures, Vol.40, pp. 1907-1921.

Zhu, J.C., Ben Bettaieb, M. and Abed-Meraim, F., 2020, "Comparative study of three techniques for the computation of the macroscopic tangent moduli by periodic homogenization scheme", Engineering with Computers, Vol.38, pp. 1365-1394.

7. RESPONSIBILITY NOTICE

The authors are the only responsible for the printed material included in this paper.